Manufacturing of agarose-based chromatographic adsorbents – effect of ionic strength and cooling conditions on particle structure and mechanical strength

Journal Item

Manufacturing of agarose-based chromatographic adsorbents – Effect of ionic strength and cooling conditions on particle structure and mechanical strength

Nicolas Ioannidis*, Andrzej Pacek, Zhibing Zhang, James Bowen

Chemical Engineering, The University of Birmingham, Edgbaston, Birmingham, B15 2TT, UK

*Corresponding author, present address: New Jersey Institute of Technology, Otto H. York department of Chemical, Biological and Pharmaceutical Engineering, University Heights, GITC Building, Suite 3901, Newark NJ 07102, USA, Tel. (+1) 201 973 596 6092, Fax (+1) 201 973 596 4594, email: nikolaos.ioannidis@njit.edu

Abstract

The effect of ionic strength of agarose solution and quenching temperature of the emulsion on the structure and mechanical strength of agarose-based chromatographic adsorbents was investigated. Solutions of agarose containing different amounts of NaCl were emulsified at elevated temperature in mineral oil using a high-shear mixer. The hot emulsion was quenched at different temperatures leading to the gelation of agarose and formation of soft particles. Analysis of Atomic Force Microscopy (AFM) images of particle surfaces shows that pore size of particles increases with ionic strength and/or high quenching temperature. Additionally it has been found that the compressive strength of particles measured by micromanipulation also increases with ionic strength of the emulsion and/or high quenching temperature but these two parameters have ~~practically~~ no significant effect on the resulting particle size and ~~/~~particle size distribution. Results from both characterization methods were compared with Sepharose 4B, a commercial agarose-based adsorbent. This is the first report examining the effect of ionic strength and cooling conditions during manufacturing, on the microstructure of micron-sized agarose beads for bioseparation.

Keywords: agarose beads; microstructure; pore size; mechanical properties; AFM; micromanipulation

1. Introduction

Agarose is one of the two constituents of agar (the other being agaropectin) which is extracted from red algae [1]. It is a linear polysaccharide consisting of 1, 3-linked β-D-galactopyranose and 1, 4-linked 3, 6-anhydro-α-L-galactopyranose, while agaropectin is a more complicated polysaccharide containing sulphuric and uronic acid residues [2]. The gelation of agarose involves a change from a random coil in solution to a double helix in the initial stages of gelation and then to bundles of double helices in the final stage [3]. The gel is formed when an ~~infinite~~ extensive three-dimensional network of agarose fibres (consisting of helices) develops [4]. At this state the material is characterized by a co-continuous macroporous morphology with polymer-rich regions (fibres) and solvent-rich regions (pores holding water), and therefore the gelation can be interpreted as a phase separation [5].

Because of its physical and chemical stability, neutral charge, hydrophilic character, open structure [6, 7] and biocompatibility, agarose has been extensively used in chromatographic separation of biomolecules [8], cell microencapsulation [9] and food additives [10]. Following functionalization with the appropriate chemistry a selective porous adsorbent can be produced for the purification of biomolecules both in packed beds and, after inclusion of densifiers, in fluidized beds [11]. The efficiency of purification depends both on macro- and microscopic properties of adsorbent. Macroscopic properties such as particle size/size distribution, shape and mechanical strength have a critical effect on throughput, pressure drop and mechanical stability of adsorbent [12]. Particles must also be sufficiently strong to withstand a number of high intensity post-manufacturing processes such as functionalization, filtration, centrifugation, sieving, pumping and washing [13]. It is therefore crucial to gain an understanding of their mechanical properties and how these are affected by manufacturing/processing conditions.

Agarose-based adsorbents with defined particle size/size distribution, mechanical properties and internal structure can be manufactured by several methods including, i) pressing the gelling polymer through a membrane [1], ii) spray gelation [14], or iii) agitation-induced emulsification of agarose solution in mineral oil [11, 15]. In this work, particles were manufactured using a high shear mixer in batch mode. Gelation of agarose and the formation of soft particles were achieved by discharging the emulsion into a separate vessel containing a large volume of mineral oil at various quenching temperatures. In this way, a wide range of cooling conditions was tested.

The important issue addressed in this paper is the effect of two processing conditions, namely ionic strength of the agarose solution and cooling conditions of the emulsion, on the microstructure and mechanical properties of agarose-based adsorbents. Microscopic properties such as mean pore size determine the maximum size of molecules that can be separated. Pore size distribution determines the available surface area for adsorption and the resolving power of the adsorbent. It has been reported that for a given concentration of agarose in the gel, pore size in gel electrophoresis slabs depends on ionic strength ~~-~~of the agarose solution [16, 17]. Despite the use of ionic strength for controlling the pore size in gel electrophoresis no extension of this has being reported for agarose, a commercially significant hydrocolloid, in *micron-sized* beads for bioseparations. Instead, agarose structure in chromatographic adsorbents is typically controlled by changing the concentration of agarose in the gel. This type of structural control presents two issues: first, a limited number of structures can be manufactured in this way and second, when wide structures are required this is at the expense of mechanical strength, although the latter issue can be overcome to a certain extent by chemical cross-linking. In addition, it is reported that cooling conditions have an effect on the structure of gel slabs for electrophoresis [18]; however cooling conditions and their effect on the structure during the formation of agarose gels have been ignored in a number of publications. Furthermore, there has been no investigation of the effect of cooling conditions on the structure of *micron-sized* agarose-based chromatographic adsorbents. This work attempts to fill this long-existing gap.

The sensitive nature of beaded agarose dictated the selection of the characterization methods employed. A number of methods exist for the structural characterization of porous materials, deriving from classical adsorption science (e.g. mercury intrusion porosimetry, nitrogen sorption). Because these methods require dewatering of the sample, they cannot be used on agarose since upon drying the soft structure of the material will collapse and information about internal structure is lost. Thermoporometry by differential scanning calorimetry, based on the melting point depression of water in the pores, cannot be used for beaded material as it is difficult to distinguish between the large melting peak of water around the particles and the small melting peak of water inside the pores of the particles [19].

The porous structure of the adsorbent was examined by Atomic Force Microscopy under an aqueous environment and also by cryo-Scanning Electron Microscopy. AFM was employed since it requires practically no sample preparation, thereby minimizing any possible distortion of the gel structure. Using this method, only the surface of the particles was examined, as it proved difficult to produce thin slices out of 50 μm particles. Cryo-SEM allowed the examination of the internal structure of the particles by freeze-fracturing, but the harsh conditions of sample preparation and examination proved unsuitable for a sensitive material such as agarose, thereby making quantification difficult. However, an important conclusion about the internal structure of the particles can be made from the cryo-SEM images acquired and this is discussed in conjunction with the information obtained from the AFM images. To examine the mechanical properties of the adsorbent, a micromanipulation technique enabling the compression of single micro-particles was employed.

2. Materials and Methods

2.1. Experimental Rig

Emulsification was carried out with a Silverson high-shear mixer (L4 series, Silverson, UK) fitted eccentrically into a stainless steel jacketed vessel with no baffle (internal diameter: 0.1 m, height: 0.15 m, V≈ 1 L). The stator (diameter: 0.026 m, height: 0.017 m, gap size: 0.175 mm) was the standard emulsor screen. Temperature was controlled with a water bath (Grant Instruments, UK) connected to the heating jacket of the vessel. Quenching was accomplished by quickly discharging the hot emulsion, using compressed air, from the emulsification vessel to a glass jacketed vessel containing 3.8 L of mineral oil. Quenching temperature in this vessel was controlled with a second water bath. During and after discharge the dispersion was mixed with a six-blade 45° pitched blade impeller. Temperature was measured in both vessels using two separate J-type thermocouples (Radleys, UK).

2.2. Materials

High-melting agarose D5 (M_w = 120 kg mol^{-1}, gelation temperature 46°- 52° C, $\rho_{(dry)}$ = 1640 kg m^{-3}) supplied by Millipore was used to manufacture the adsorbent particles by a hot emulsification method and white mineral oil Marcol N82 ($\rho_{(90^\circ C)}$ = 812 kg m^{-3}) (ESSO, UK) was used as the continuous phase. Sodium chloride (Sigma Aldrich, UK) was used as a co-solute for controlling the ionic strength of the agarose solution and the pore size of the adsorbent. Oil – soluble Span 85 (sorbitan trioleate, hydrophilic – lipophilic balance (HLB): 1.8, $\rho_{(20^\circ C)}$ = 956 kg m^{-3}, M_w = 975.51 g mol^{-1}) (Sigma Aldrich, UK) was used to stabilise the emulsion and control particle size.

Agarose powder at a concentration of 4 % (w/w) was dissolved in a solution of NaCl in distilled water at 90° C whilst stirring. When the solution became fully transparent it was placed in a water bath at the same temperature where it was held for at least 30 min to enable full de-aeration. Distilled water was added to account for water loss during the holding period.

2.3. Emulsification

Mineral oil (800 mL) and Span 85 (8 mL - 0.1 % (v/v of oil)) were charged into the emulsification vessel. The mixture was equilibrated at 90° C while stirring at 1000 rpm for about 30 min. Agarose solutions (200 mL) containing different amounts of salt (no salt, 0.01, 0.025, 0.05 and 0.1 molal (m)) were injected into the mineral oil using a preheated syringe (to avoid gelation). After 5 min of shearing at 3500 rpm the emulsion was discharged using compressed air (0.5 bar) into the cooling vessel in which 3.8 L of oil were stirred at 300 rpm at various quenching temperatures (0°, 10° and 20° C).

2.4. Particle separation

After gravitational separation, concentrated oil-particles mixture was centrifuged (Thermo Fisher Scientific, UK) at 3000 rpm (1830 g) for 10 min to separate the particles from the oil. Residual oil was removed from the surface of the particles by washing with ethanol/water solutions of increasing (1:9, 3:7, 5:5, 7:3, 9:1 (v/v)) following decreasing (9:1, 7:3, 5:5, 3:7 (v/v)) concentrations to prevent structural damage from rapid dehydration [20]. After washing, particles were kept in 25 % (v/v) aqueous ethanol solution to prevent bacterial contamination.

2.5. Particle sizing

Particle size distributions were measured with the Mastersizer 2000 (Malvern, UK). Mean particle size of samples ranged between 45-55 µm. Because the emulsion was stabilized by surfactants, changing of the ionic strength of the agarose solution or quenching temperature has practically no effect on the resulting particle size/size distribution.

2.6. AFM and cryo-SEM sample preparation

AFM images were acquired using a MultiMode AFM (Veeco, UK) housed on a vibration isolation table. Nanoscope v5.12 software (Veeco, UK) was used throughout for both real-time analysis and post-capture image processing. A drop of particle aqueous suspension (70 % (v/v)) from each sample was immobilized on a glass slide using double-side tape. All images were acquired while operating in Tapping Mode under ambient conditions, using rectangular 180 µm length pyramidal-tipped Si cantilevers (Veeco, UK) with nominal spring constants of 40 N m^{-1} and resonant frequencies in the range 250-350 kHz. The AFM piezoelectric tube scanner had a maximum lateral range of 14 µm x 14 µm and a maximum vertical range of 1.9 µm when operating in Tapping Mode. All images were acquired at scan rates between 0.5-1.5 Hz, each image being composed of 512 x 512 pixels. Each sample was examined for up to 20 min to ensure drying of the gel network did not occur. Later visual examination of the film confirmed that particles were still wet.

To obtain information on the internal structure of particles, samples were examined with a Philips XL 30 FEG ESEM microscope operating in SEM mode. A drop of particle aqueous suspension (70 % (v/v)) from each sample was placed on a brass stage mounted on a steel rod. The rod was immersed in nitrogen slush (-140° C) and then quickly transferred to the SEM preparation chamber. Samples were fractured using a metal rod accessing the preparation chamber. After freeze-fracturing the sample was sublimated (etched) at -90° C and $4 \bullet 10^{-5}$ mbar of vacuum for 8 mins. After etching the temperature was lowered back to -140° C. Finally a platinum coating (1 min exposure, thickness 5 nm) was applied on the surface of the sample in order to prevent damage by the electron beam. After sample preparation the rod was transferred from the preparation chamber to the interconnected examination chamber. An electron beam of 10 keV was used at $4 \bullet 10^{-5}$ mbar of vacuum and -140° C, for the examination of agarose particles.

2.7. Micromanipulation compression method

The mechanical properties of particles were measured using a micromanipulation technique. In this technique, described in detail elsewhere [21], a single particle is compressed between two parallel plates with accurate measurement of the compressive force and the corresponding particle displacement. Two sets of experiments were carried out. In the first set, particles were compressed to 30% final deformation (defined as the ratio of displacement to the diameter of an undeformed particle) to determine the deformation at which particles were fully elastic and to calculate Young's modulus of the particles. In the second set, the viscoelastic properties of the particles were determined from compress/holding experiments.

3. Results and Discussion

3.1. Characterization by AFM

3.1.1. Effect of ionic strength of agarose solution on pore size/pore size distribution

Fig. 1a and Fig. 1b show the effect of ionic strength expressed by the molal concentration of NaCl on the structure of agarose particles for the control sample (no salt) and the highest NaCl concentration used (0.1 m). For an electrolyte consisting of monovalent ions, such as NaCl, its molal concentration also expresses its ionic strength. Therefore, in the results presented below the molal concentrations of NaCl mentioned, also express the ionic strengths of the agarose solution. 'Pores' were considered the darkest spots (dark brown colour) on the AFM images (500 measurements from each sample). These spots are roughly circular and their diameter appears to increase linearly with ionic strength especially for the highest ionic strength used (0.1 m). In addition, as the diameter of pores increases, the number of pores per unit area reduces. Fig. 2a and Fig 2b show the measured mean pore size and pore size distribution respectively, of samples manufactured with increasing ionic strength. No significant difference in mean pore size was observed between pure agarose and sample containing 0.01 m NaCl (38 nm (standard error 0.92 nm) and 40 nm (standard error 0.98 nm), respectively). However, when NaCl concentration was increased from 0.01 m to 0.1 m, up to almost five-fold increase in mean pore size was observed (from 40 nm to 190 nm). Since agarose concentration in the gel was the same for all samples the results suggest that increase in pore size is caused by changes in the conformational arrangement of the agarose fibres. It is worth noting that apart from an increase in mean pore size with ionic strength, a significant increase in the span of the pore size distribution was also observed (Fig. 2b).

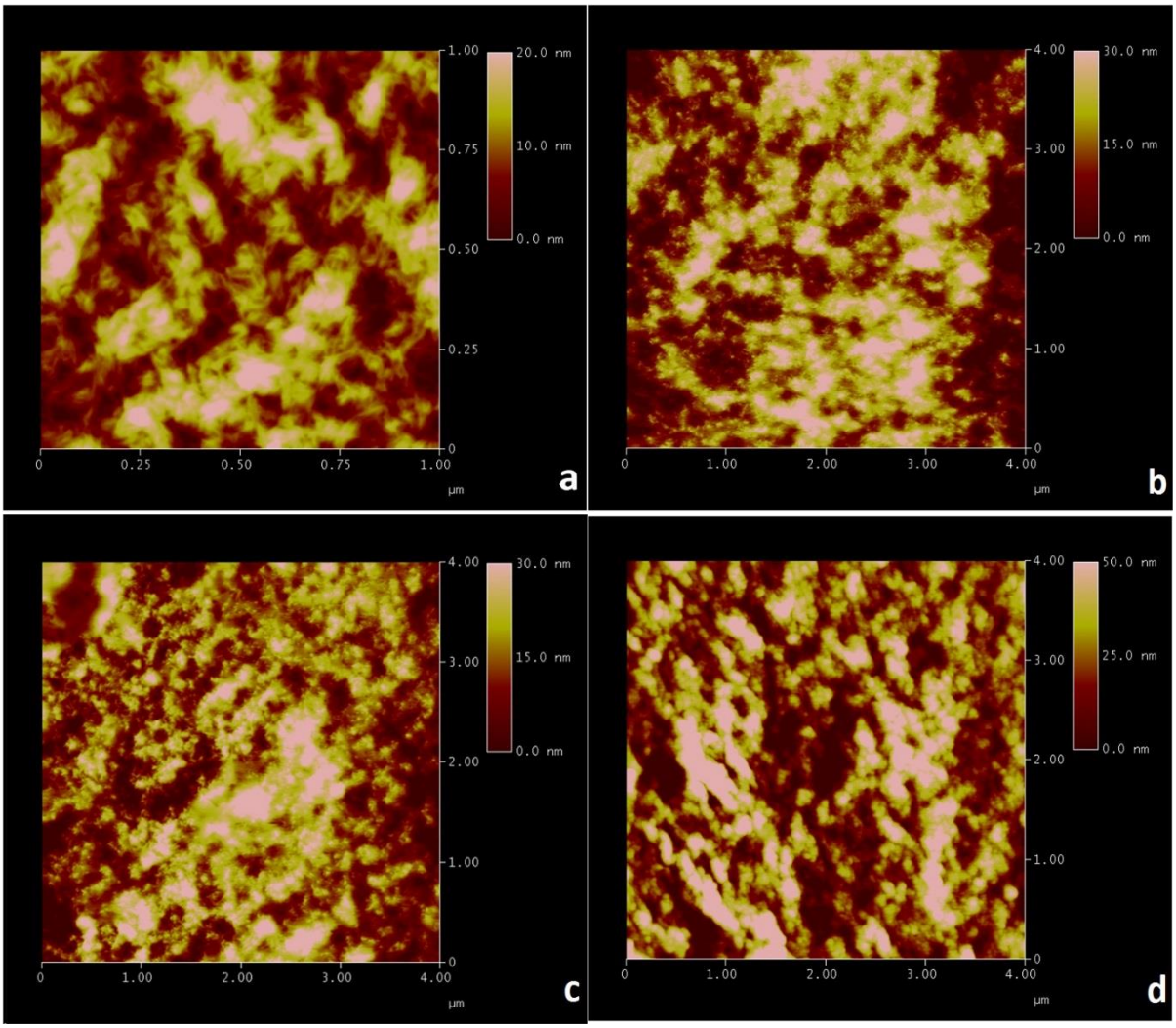

Figure 1. *Example of the effect of ionic strength on the pore structure of agarose beads (quenched at 0° C), (a) 0 m, mean pore size 38nm, (XY: 1 µm, Z: 20 nm), (b) 0.1 m, mean pore size 190 nm (XY: 4 µm, Z: 30 nm). Example of the effect of quenching temperature on pore structure (ionic strength: 0.05 m) (c) 0° C, mean pore size 128 nm, (XY:*

4µm, Z: 30 nm), (d) 20° C, mean pore size 195 nm (XY: 4 µm, Z: 50 nm), note: X and Y are the horizontal and lateral distances of the scan respectively, therefore indicating the scale of the image.

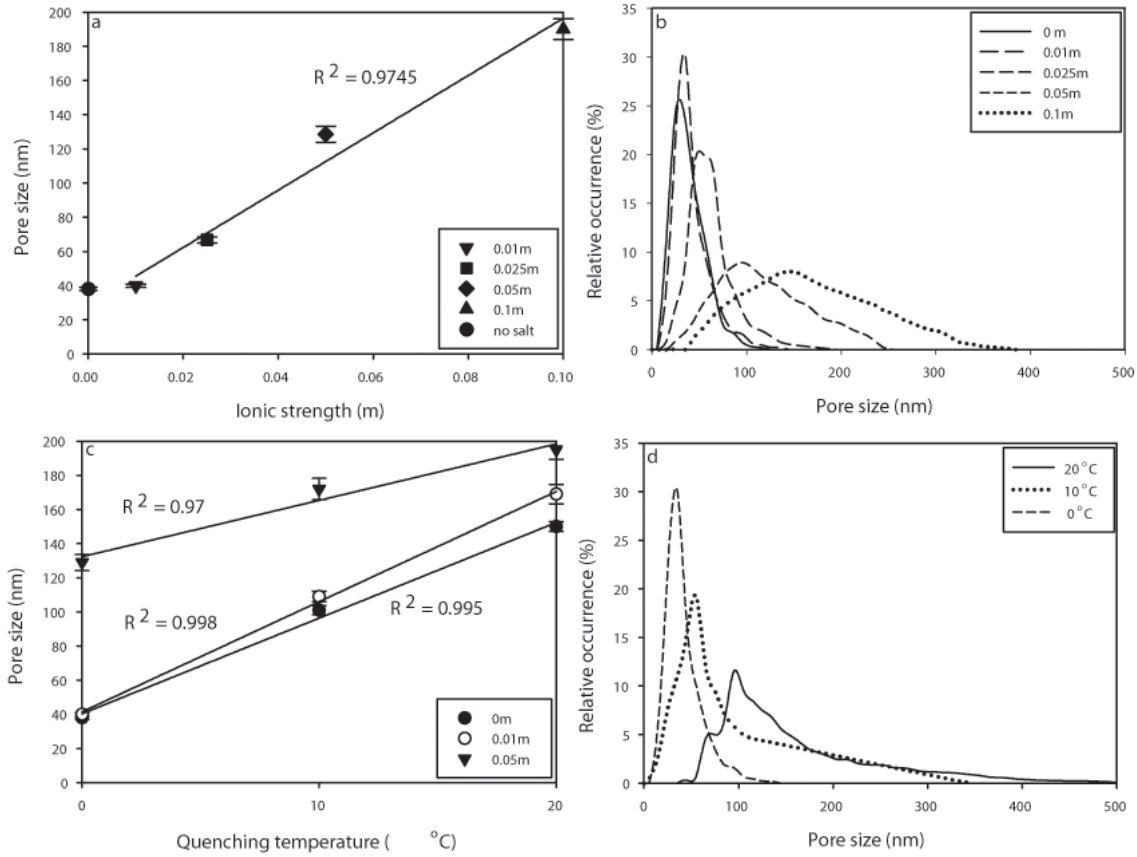

Figure 2. *(a) Mean pore size as a function of ionic strength, (b) pore size distribution as a function of ionic strength, quenching temperature: 0° C, (c) mean pore size as a function of quenching temperature at different ionic strength, (d) pore size distribution as a function of quenching temperature, ionic strength: 0.01 m, bin size for both distributions: 10 nm, error bar indicate the standard error of the mean.*

Despite different concentrations of solute (agarose) and co-solute (NaCl), type of co-solute, gel casting/setting conditions and characterization methods, similar results about the effect of ionic strength on pore size of agarose gels have been reported in the literature. However, this is the first account in the open literature of examining this effect on the pore properties of *micron-sized agarose beads*. Attwood *et al.* [22] by means of electron microscopy reported an average pore size of 37 nm for beaded agarose of 4% (w/w) containing no salt. This correlates well with the control sample and the sample of lowest ionic strength (0.01 m) manufactured in this work that had 38 nm and 40 nm pore size, respectively. Maaloum *et al*. [17] studied the effect of concentration of TBE (Tris borate ~~E~~ethylenediaminetetraacetic acid) buffer on agarose gel slabs using AFM, obtained images of similar quality and interpreted data in the same way as in this work (diameter-based measurements of circular dark spots on the AFM images). They reported an increase in pore size and in the span of the pore size distribution with ionic strength of the agarose solution. Serwer and Griess [16] studied the effect of various buffers on the structure of agarose slabs designated for electrophoresis and reported an increase in mean pore size with ionic strength. Waki *et al*. [23], studied agarose gels formed in the presence of TBE buffer using electron microscopy of freeze dried samples. Although the quality of their images was poor they concluded that agarose fibres tend to aggregate in the presence of salts thus producing gels with large pore size and wide size distribution. In these studies the researchers confirmed their results with electrophoretic measurements concluding that the relative migration rates of DNA plasmids substantially increased when salt was present in the gel.

The results presented above can be explained by the salting-out effect. When a biopolymer is dissolved in an aqueous solution, water molecules tend to create a hydration envelope around the dissolved chains through solvent-solute hydrogen bonding. When salt is added, the preferential hydration of the salt ions over the

biopolymer chains tends to reduce the size of this envelope [24]. This salt-induced dehydration promotes chain-chain interaction and ultimately chain aggregation during gelation. Since agarose concentration is the same in all samples, upon the addition of salt, a gel with larger pore size and consequently thicker fibers ~~is~~are formed, compared to gelation in a salt-free solution. The extent of the salting-out effect depends on the ionic strength of the solution and not on the type of salt used [25]. This effect also accounts for the wide pore size distribution. Fig. 2b shows that the distribution of pores in the gel has increased toward the larger size of the graph (right-hand side) indicating greater number of large-sized pores. This is probably because during gelation and fiber aggregation of the salt-containing solution, thicker or larger fibres have more sites available for intermolecular entanglement, thus will aggregate to a larger extent than thinner or smaller fibers upon the addition of salt.

3.1.2. Effect of quenching temperature of agarose solution on pore size/pore size distribution

Fig. 1c and Fig 1d shows the effect of quenching temperature on the structure of agarose particles quenched at 0° C and the sample quenched at 20°C (ionic strength for both: 0.05 m). Mean pore size (Fig. 2c) appears to increase linearly with higher quenching temperature (slower cooling) for all three ionic strengths used. This suggests that quenching temperature (cooling conditions) has a significant effect on the conformation of the agarose fibres. Fig. 2d shows the pore size distribution of these samples. At high quenching temperature an increase in the span of the distribution of pore size is also observed. In fact, the resemblance between the pore size distributions in Fig. 2b and Fig. 2d indicates a similarity between the effect of cooling conditions and ionic strength on the structure of agarose. The latter suggests that structurally identical gels can be manufactured from different sets of conditions. The regression lines for 0 m and 0.01 m in Fig. 2c suggest that cooling conditions are the predominant factor in changing the conformation of the agarose fibres in the gel, compared to ionic strength. In the control and 0.01 m sample no difference in pore size is observed with fast cooling (0° C), whereas at high quenching temperature (10 and 20° C) the difference in pore size between the two samples becomes more significant. A phenomenon that was not observed with increasing ionic strength for the lowest quenching temperature was the increase of the roughness of the sample surface, as indicated by the ~~(~~Z-range in the AFM images~~,)~~ with increasing quenching temperature. In particular, samples quenched at 0° C had an average surface roughness of 30 nm whereas the respective value for samples quenched at higher temperatures (10° and 20° C) was between 50 and 100 nm, again indicating the predominance of the effect of cooling conditions over ionic strength on the agarose structure.

In a simplistic way, one could argue that high quenching temperature allows more time for the gel network to develop. Thus fast cooling will result in a gel network that is closer to the solution state of agarose (poor phase separation), whereas slow cooling results in a well-developed network with thicker agarose fibres and larger pores holding water. The different conformational arrangement of the agarose fibres during gelation is also indicated by the difference in roughness between samples manufactured at different cooling conditions.

The increases in mean pore size and span of the pore size distribution of agarose gels with quenching temperature found in this work are in good agreement with the literature. The effect of cooling temperature on the structure of agarose gels has been previously studied on centimetre-sized gel slabs using a variety of techniques including absorbance measurements [26] and electrophoresis [18]. Despite that, this is the first account in the literature relating cooling conditions to the pore size of *micron-sized* agarose beads. All of the above researchers reported an increase in mean pore size of agarose gels with slow cooling, while the last [18] also reported an increase in the span of the distribution of pore sizes as well as differences in the melting profiles (measured by differential scanning calorimetry) of gels cooled at different final temperatures.

3.1.3. Internal structure of particles by cryo-SEM

In this work, AFM was employed as a surface technique to study the effect of processing conditions on the pore size/size distribution of the adsorbent. Therefore deductions about the internal structure of the particles cannot be made alone from the AFM results. To obtain information on the internal structure, particles were examined using cryo-SEM. Unfortunately, upon freezing-fracturing of particles, crystal formation was detected in various locations of the samples which distorted the agarose structure. In addition, whenever salt was present in the formulation, it precipitated on the gel network during etching. Because of this, quantitative characterization from the SEM images was difficult. However, the following important conclusion can be drawn from these images:

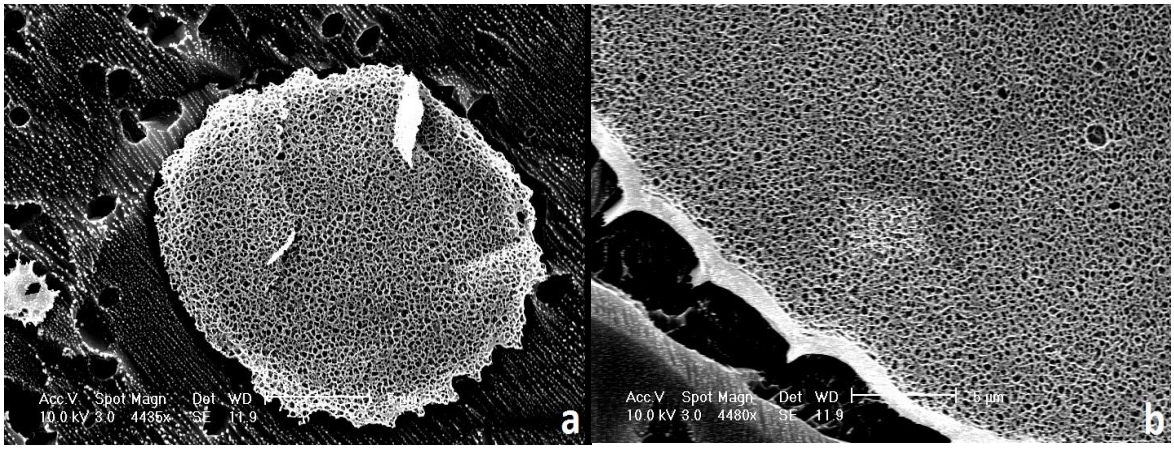

Figure 3. *(a) Cross-section of 15 µm ~~in~~ diameter particle (b) Cross-section of 100 µm ~~in~~ diameter particle. (Both quenched at 20°C, ionic strength 0 m).*

In Fig. 3a it is evident that the structure of the agarose gel network is uniform throughout the entire cross-section of the particle, i.e. no pore size gradients have been formed during manufacturing. This homogeneity has beening observed in cryo-SEM images of all samples manufactured in this work (other formulations not shown). More importantly, in both Fig. 3a and Fig. 3b the size of pores observed in various locations on the samples is practically identical to the size of pores located near the surface of the particles (the white non-porous layer around the surface of the cross-section of the particle in Fig 3b is an ice artefact. This is evident by the fact that the particles from this sample have a surface mean pore size of 150 ± 3 nm as observed with the AFM). This suggests that the values of size/size distribution of pores obtained from AFM images and reported in Fig.2a-2d represent the pore size/size distribution in the interior of the particles. Therefore, any assumptions made about the pore size/size distribution, based on the AFM images, can be extended to the internal structure of the particles.

3.1.4. Comparison with commercial Sepharose 4B and Sepharose CL - 4B

The porous structure of particles manufactured in this work was compared against Sepharose 4B and Sepharose CL-4B. The mean pore sizes of Sepharose 4B and Sepharose CL-4B (51 ±1 nm and 42 ±1 nm respectively) as well as their pore size distributions are very similar to those of the control sample manufactured in this work (Fig. 1a, sample with no salt, quenched at 0°C). As it was noted earlier (section 3.1.1), for the range of ionic strength and quenching temperature used here, up to a five-fold increase in the mean pore size of the adsorbent was observed (from 38 nm to 195 nm). Considering that these conditions were of a specific range, it is possible that even wider structures could potentially be manufactured, reaching mean pore sizes in the micrometer range. Such structures can be advantageous in the purification of newly emerging biomolecules such as plasmids and viruses that are large in size (up to 300 nm, potentially ~~bigger~~larger) [12]. Current purification of such entities using conventional adsorbents designed and optimized for proteins, such as Sepharose 4B, results in adsorption almost exclusively on the outer surface of the adsorbent as has been observed by poor chromatographic performance [27] and confirmed by confocal microscopy [28, 29]. Although larger pore size due to extensive interfiber aggregation indicates reduction in internal surface area, an adsorbent with a very wide structure would provide larger apparent surface area for adsorption by allowing such large molecules to adsorb in the interior of the particles, thus increasing adsorption capacity and separation efficiency. Superporous agarose particles obtained by template-based, double emulsification can be used for the purification of such large bioproducts but such technology has yet to be realized commercially. Large-scale manufacturing of such macroporous adsorbents is not only complicated and expensive [12] but also the method suffers from reproducibility and the extensive post-manufacturing washing procedures to obtain the particles [30].

The practically identical porous properties of Sepharose 4B and Sepharose CL - 4B allow one to deduce that particles manufactured in this work with wide structures can be chemically cross-linked to various degrees to produce mechanically superior adsorbents while maintaining their original porous properties. The mechanical properties of Sepharose – 4B and Sepahrose CL – 4B are discussed later along with the mechanical properties of samples manufactured in this work.

3.2. Characterization of mechanical properties

3.2.1. Compression test

During the compression of particles the normal stress of the sphere is not uniform, but it varies from the maximum σ_{max} to the minimum σ_{min} in the cross-section half-way between the compressing surfaces. The full analysis of the spatial stress distribution is rather complex and in this case unnecessary, since only a comparison between samples is of interest. Therefore the compressive stress of particles was compared in terms of average stress σ_{av}, or pseudo-stress, which is defined as the ratio of the compressive force to the cross-section of an undeformed particle.

The theory for elastic spheres compressed between two flat rigid surfaces was developed by Hertz. For deformations up to 10%, the relationship between force *F* (N) and displacement *h* (m) is described by:

$$F = \left[\frac{4}{3}\frac{r^{0.5}}{2^{1.5}}\frac{E}{1-\nu^2}\right]h^{1.5} \qquad (1)$$

Where *r* (m) is the radius of the particle, *E* (Pa) is Young's modulus and ν is Poisson's ratio. At higher deformations the Hertz equation fails. An extension of the Hertz model has been developed by Tatara who introduced higher order terms in the force-displacement equation and suggested a semi-empirical relationship between force and deformation valid for up to 60 % deformation (Eq. 2) [31]. An example of experimental data from a particle of 100 µm in diameter fitted to the Tatara model can be seen in Fig. 4a.

$$F = ah^{1.5} + bh^3 + ch^5 \qquad (2)$$

Where *a, b* and *c* material-depended constants determined experimentally.

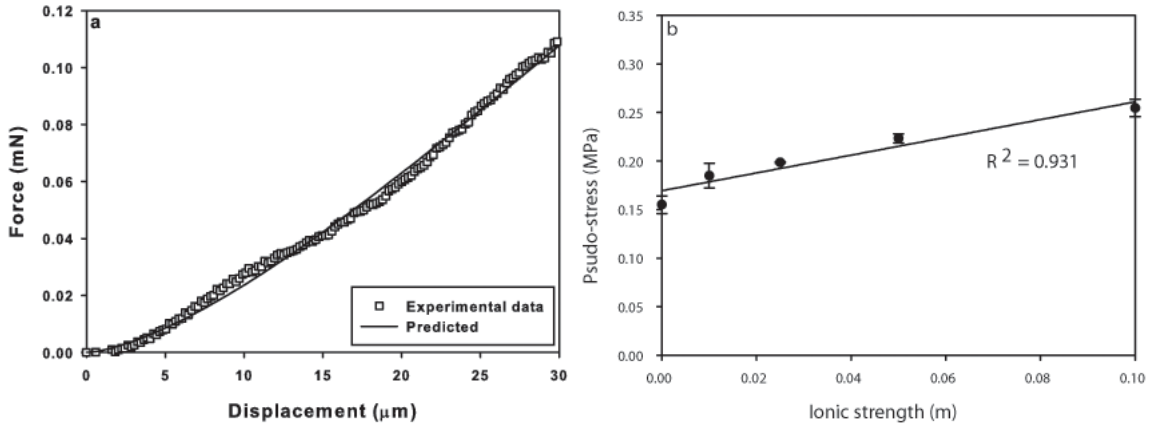

Figure 4. *(a) Example of 30% deformation for a particle of 100 µm ~~in~~ diameter (ionic strength 0.05 m, quenched at 0°C): (•) experimental data, (-) best fit to Tatara model. (b) Young's modulus of particles manufactured with increasing ionic strength using the Tatara model, error bars indicate the standard error of the mean*.

Fig 5a and Fig. 5b show the compression for up to 30 % deformation of samples manufactured with increasing ionic strength and slow cooling, respectively. Particles manufactured with increasing ionic strength show a tendency to become stiffer. For the highest ionic strength tested (0.05 m) an increase of the order of ~ 35% in compressive stress was observed. A similar tendency to become stiffer was observed for particles manufactured at high quenching temperature. An increase in compressive stress of the order of ~ 45% was observed for the sample quenched at 20°C, containing 0.05 m of NaCl, when compared to the control sample (no salt, quenched at 0°C). The values obtained for compressive stress of agarose particles was in reasonable agreement with the literature [13]. Compressive stress for up to 30% deformation of Sepharose 4B was of the same order as the control sample of this work (no salt, quenched at 0°C) (Fig. 5c). These two samples also had nearly identical pore properties as observed in their AFM images (51±1nm and 38±1nm respectively). This observation suggests a similarity between the manufacturing conditions of these two types of particles and possibly chromatographic column performance. Sepharose 4B CL yielded the largest compressive strength among the sample tested. This is because chemical cross-linking introduces inter- and intra-molecular bridges in the agarose fibres, vastly improving the rigidity of the gel [32].

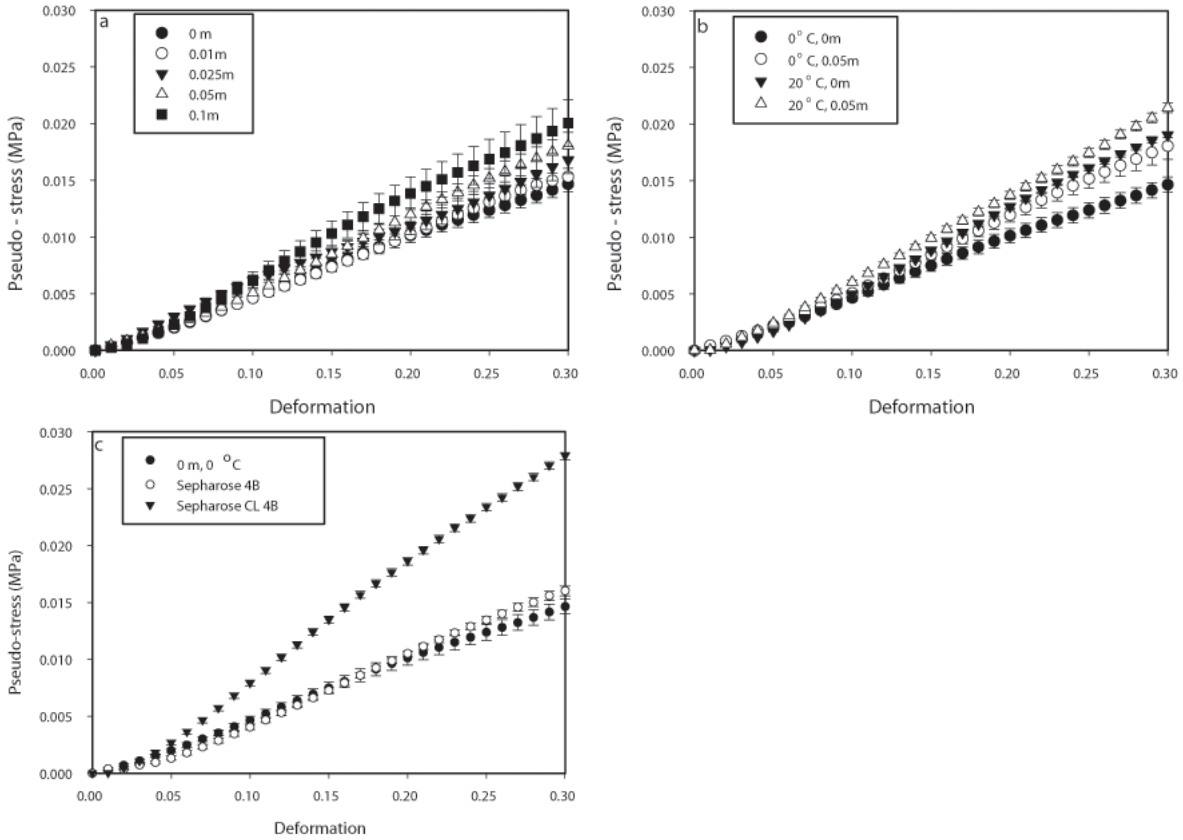

Figure 4. *Pseudo-stress vs. deformation for up to 30% of particles manufactured with (a) increasing ionic strength and (b) quenched at different temperatures, (c) pseudo-stress vs. deformation for up to 30 % of Sepharose 4B, Sepharose CL-4B and control sample (0 m 0°C), error bars indicate the standard error of the mean.*

Young's modulus of particles was calculated from large deformation data, using the Tatara model and it was in reasonable agreement with the literature [15]. For the calculation it was assumed that the Poisson ratio of the particles was 0.5 [13]. The Tatara model was used by predicting the parameters of the model using SigmaPlot (Systat Software Inc, USA). The Young's modulus of particles increased with increasing ionic strength (Fig. 4b) and high quenching temperature.

The observed increase in the compressive stress of particles manufactured with increasing ionic strength and /or high quenching temperature is directly related to the conformation of agarose fibres during gelation. For a given concentration of agarose, both high ionic strength and high quenching temperature promote fibre aggregation during gelation. As observed in the AFM images of the particles this extended aggregation results in a gel with large pore size and wide pore size distribution. The rigidity of the gel structure depends on the extent of the intermolecular hydrogen bonding between fibres [15]. Therefore any process that favours this aggregation results in a higher number of intermolecular hydrogen bonds per unit volume of the gel and ultimately to a stiff gel ~~(~~of higher Young's modulus, exhibiting a~~) with~~ large pore size.

3.2.2. Compress/hold experiments

Fig. 6a and Fig 6b show the results of compress/hold experiments for particle manufacture with increasing ionic strength and high quenching temperature, respectively. Particles were compressed up to 50% deformation and held at this position for at least 35 sec. It can be seen for particles manufactured in this work (Fig 6a-b) that there is practically no significant stress relaxation and the change is of the order of 10 % (standard error of the mean ±4.5 - 11.5 %). Sepharose 4B and Sepharose CL-4B exhibited similar behaviour to these samples. In addition, the holding part of the curve is practically parallel to the x-axis indicating mainly elastic behaviour of the particles. For this reason no viscoelastic model was used to describe this behaviour. These results indicate that no permanent changes occurred in the internal structure of the particles for up to 50 % deformation. However, it has been shown that at higher deformations (80 %) [13] particles become viscoelastic indicating permanent changes in the internal structure of particles. Therefore, for engineering calculations regarding such range of deformations and compression speeds, particles can be treated as fully elastic.

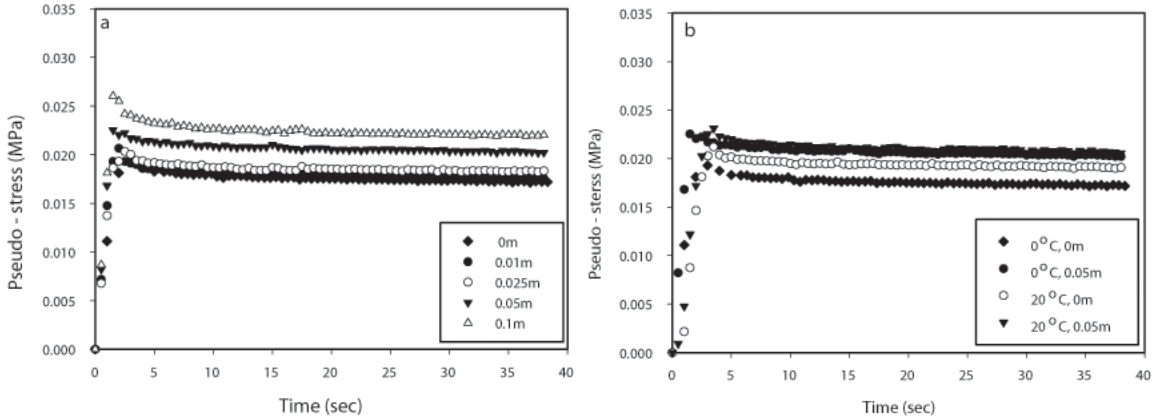

Figure 6. *Pseudo-stress vs. time obtained from compress/hold experiments: (a) samples of increasing ionic strength, quenched at 0°C, (b) samples cooled at different quenching temperatures.*

The last two sets of experiments (compress and compress/hold) provide information that has direct practical application as it can be used to determine the maximum height of the fixed bed at which the mechanical characteristics of the particles do not change. This type of information can also influence the design of industrial scale washing, filtering and sieving operations as well as the selection of procedures for transporting the product around a production plant [13].

4. Conclusion

The effect of ionic strength of the agarose solution and quenching temperature of the emulsion on the structure and mechanical strength of agarose beads for bioseparations was investigated. This is the first account of examining the effect of these two processing conditions on the microstructure of *micron-sized* agarose-based particles. AFM images of particles showed that the mean pore size of agarose beads increases with ionic strength of the agarose solution. In addition to the increase in mean pore size a span of the pore size distribution was also observed. The same structural trends were observed when the emulsion was quenched at high temperature. Overall for the range of processing conditions used in this work up to a five-fold increase in pore size was observed. The determination of the mechanical properties of particles prepared in this work showed that the widening of the agarose structure is accompanied by an increase in particle stiffness. This is reasonable since the rigidity of the agarose gel depends on the extent of intermolecular hydrogen bonding between fibres and consequently, since both ionic strength and slow cooling promote the latter, an increase in the stiffness of particles is observed. The range of processing conditions used to control the micro-structural properties of the beaded adsorbents did not appear to affect particle size/ size distribution. This suggests that this type of structural control can be applied during manufacturing with minimal impact on the overall process. This work contributes to the understanding of the micrometer-range structural behaviour of beaded agarose, a commercially significant hydrocolloid, during the manufacturing process. The results presented in this paper can be used to optimize the large-scale manufacturing process of agarose beads by the selecting the appropriate ionic strength of the agarose solution and quenching temperature of the emulsion. The results may be further exploited to inexpensively prepare agarose beads of tailored structural characteristics with better performance than commercially available ones for industrial applications, particularly for the purification of large-sized bioproducts.

Acknowledgements
The authors received financial support from EPSRC and Millipore, UK

Appendix A. Nomenclature

a: coefficient of Hertz equation
b, c :material depended constants
E: Young's modulus (Pa)
F: force (N)
g: gravitational acceleraion (m/s^2)
h: height (m)
M_w: molecular weight ($kg\ mol^{-1}$)
r: particle radius (m)
R_c: radius of curvature (m)

Greek symbols:

v: Poisson ratio
σ: stress (Pa)

References

[1] Q.-Z. Zhou, L.-Y. Wang, G.-H. Ma, Z.-G. Su, J. Colloid Interface Sci. 311 (2007) 118.
[2] Araki, Bull. Chem. Soc. Jpn. 29 (1956) 43.
[3] K.B. Guiseley, Enzyme Microb. Technol. 11 (1989) 706.
[4] V. Normand, D.L. Lootens, E. Amici, K.P. Plucknett, P. Aymard, Biomacromolecules 1 (2000) 730.
[5] E. Pines, W. Prins, Macromolecules 6 (1973) 888.
[6] S. Hjertén, J. Chromatogr., A 61 (1971) 73.
[7] J. Gutenwik, B. Nilsson, A. Axelsson, AIChE J. 50 (2004) 3006.
[8] A. Jungbauer, J. Chromatogr., A 1065 (2005) 3.
[9] H. Uludag, P. De Vos, P.A. Tresco, Adv. Drug Delivery Rev. 42 (2000) 29.
[10] L.M. Barrangou, C.R. Daubert, E. Allen Foegeding, Food Hydrocolloids 20 (2006) 184.
[11] M. Jahanshahi, Andrzej W Pacek, Alvin W Nienow, Andrew Lyddiatt Journal of Chemical Technology & Biotechnology 78 (2003) 1111.
[12] A. Lyddiatt, Curr. Opin. Biotechnol. 13 (2002) 95.
[13] Y. Mu, A. Lyddiatt, A.W. Pacek, Chem. Eng. Process. 44 (2005) 1157.
[14] A.M. Egorov, A.K. Vakhabov, V.Y. Chernyak, J. Chromatogr., A 46 (1970) 143.
[15] Y. Yan, Z. Zhang, J.R. Stokes, Q.-Z. Zhou, G.-H. Ma, M.J. Adams, Powder Technol. 192 (2009) 122.
[16] P. Serwer, Griess, Gary A., in: (Ed.)^(Eds.), U.S.A, 1991.
[17] M. Maaloum, N. Pernodet, B. Tinland, Electrophoresis 19 (1998) 1606.
[18] N. Kusukawa, M.V. Ostrovsky, M.M. Garner, Electrophoresis 20 (1999) 1455.
[19] R.J.H. Stenekes, S.C. De Smedt, J. Demeester, G. Sun, Z. Zhang, W.E. Hennink, Biomacromolecules 1 (2000) 696.
[20] A. Amsterdam, Z. Er-El, S. Shaltiel, Arch. Biochem. Biophys. 171 (1975) 673.
[21] G. Sun, Zhang, Z., J. Microencapsulation 18 (2001) 593.
[22] T.K. Attwood, B.J. Nelmes, D.B. Sellen, Biopolymers 27 (1988) 201.
[23] S. Waki, J.D. Harvey, A.R. Bellamy, Biopolymers 21 (1982) 1909.
[24] B.J. Bowman, Ofner III, Clyde M., Schott, Hans, in: D.B. Troy, (Ed.)^(Eds.)Remington: The Science and Practice of Pharmacy, 21 ed.; Lippincott Williams & Wilkins, 2005, p 299.
[25] T.G. Park, A.S. Hoffman, Macromolecules 26 (1993) 5045.
[26] N. Janaky, et al., J. Phys. Confer. Series 28 (2006) 83.
[27] I. Theodossiou, M. Søndergaard, O.R.T. Thomas, Bioseparation 10 (2001) 31.
[28] A. Ljunglöf, P. Bergvall, R. Bhikhabhai, R. Hjorth, J. Chromatogr., A 844 (1999) 129.
[29] E. Thwaites, S.C. Burton, A. Lyddiatt, J. Chromatogr., A 943 (2002) 77.
[30] A.K. Maria B. Dainiak, Igor Yu. Galaev, and Bo Mattiasson, Macroporous Polymers: Production Properties and Biotechnological/Biomedical Applications. 1st ed., CRC Press Taylor & Francis Group, Boca Raton, 2009.
[31] P. Ding, I.T. Norton, Z. Zhang, A.W. Pacek, J. Food. Eng. 86 (2008) 307.
[32] J. Porath, T. L»»s, J.-C. Janson, J. Chromatogr., A 103 (1975) 49.